Electronic Supplementary Material (ESI) for Physical Chemistry Chemical Physics

Photoelectrooxidation of Water on Hematite Thin Films

I. Herrmann-Geppert[a], P. Bogdanoff[a], S. Fengler[b], T. Dittrich[b] and S. Fiechter[a]

[a] Institute for Solar Fuels, Helmholtz-Zentrum Berlin für Materialien und Energie, Hahn-Meitner-Platz 1, 14109 Berlin, Germany
[b] Institute for Heterogeneous Materials, Helmholtz-Zentrum Berlin für Materialien und Energie, Hahn-Meitner-Platz 1, 14109 Berlin, Germany

α-Fe_2O_3 (hematite) photoanodes for the oxygen evolution reaction (OER) were prepared by a cost-efficient sol-gel procedure. We show that annealing and plasma post-treatments improve significantly the photoelectrochemical properties for the OER. Annealing steps lead to a reorganization of the crystal structure and thereby to a pronounced shift of the photocurrent to negative potentials. Surface photovoltage measurements (SPV) indicate an enhanced separation of charge carriers originated from the band gap photoabsorption. Nevertheless a more pronounced effect on the catalytic efficiency was gained by a surface-treatment in oxygen plasma. X-ray photoelectron spectroscopy (XPS) analysis reveals an oxygen enriched surface layer with new oxygen species which might be responsible for the improved electrochemical activity. SPV measurements identify an increased fraction of transferred charge carriers from this newly produced surface defects. The combination of these post-treatments leads finally to an efficient hematite photoanode for the OER.

Introduction

Photo-induced water splitting is seen as a clean and renewable energy resource to produce hydrogen as a fuel. That is why photoelectrochemical research is focused on the development of devices for the solar fuel generation. In such a system, a photoactive material generates charge carriers by the visible light absorption which can participate in the redox reaction of water on the catalytic surface. Nevertheless the overall efficiency of such a device is limited to the slow water oxidation reaction.

Semiconducting α-Fe_2O_3 (hematite) is discussed as a promising electrode material for the photo-induced water oxidation reaction (1, 2). It reveals a suitable direct band gap of 2.2 eV for the visible light absorption and the valence band position is more positive with respect to the redox potential of the water oxidation reaction. The material, however, possesses a low charge carrier mobility and short hole diffusion length which lead to a high rate of recombination before the charge carriers can be involved in electrochemical reactions at the electrode/electrolyte interface. In the literature it is reported that these drawbacks can be surmounted by the introduction of dopants in the semiconductor crystal lattice (e.g. 3, 4). Furthermore, the reaction rate or catalytic activity towards water oxidation is low but can be accelerated by the deposition of highly efficient noble metal-containing co-catalysts (e.g. IrO_2) on the Fe_2O_3 surface (1).

In our recent contribution (5), we have demonstrated that the obtained photovoltage and the photocurrent density of sol-gel prepared hematite thin layers can be significantly enhanced by an oxygen plasma and/or an annealing treatment of the pristine material. It was suggested that recombination centers were diminished by a re-crystallization process of the hematite particles and that their surface chemistry was modified by the plasma treatment in a beneficial way with respect to higher reaction rates towards the water oxidation reaction.
The work presented here establishes our recent work and elaborates the post-treatment effects on the hematite films in more detail. The post-treatment procedures have been closer investigated, especially in terms of the structural changes of the films. Surface photovoltage measurements will elucidate the improved charge carrier dynamics after the post-treatment application.

Experimental methods

The preparation of the films is described in detail in Ref. (5). Briefly summarized, nanocrystalline hematite films were obtained by a sol-gel procedure adapted to the Pecchini method (6). Iron nitrate was introduced in a polymer network gained from the gelation of citrid acid and ethylenglycol. The resin-type sol-gel was deposited on fluorine-doped tin-oxide glasses (FTO) by dip coating. Afterwards the films were calcinated in air atmosphere at 500 °C.

Post-treatments of the films

Plasma treatment was performed in a plasma etcher by Diener electronics at the Optotransmitter Umweltschutz Technologie e.V. (OUT e.V. Berlin). The films were placed in the reaction chamber with their conducting side face upwards. The chamber was evacuated until an oxygen partial pressure of 0.2 mbar was reached. In the presented experiment gas flow of 20 sccm was established. The sample was treated for 20 min in the plasma.

For the post-annealing in an oxygen gas flow, the sol-gel process prepared hematite films were placed in a quartz tube of a split-hinge furnace again. The tube was connected to the oxygen gas supply so that a flowing oxygen gas atmosphere was established within the tube. The temperature was increased up to 500 °C with a heating rate of 1 K/min and held at this temperature for two hours.

For the post-treatment with successive steps the annealed hematite film was treated in the oxygen plasma for 5 min.

Electrochemical characterization

Electrochemical measurements were performed in a three-electrode compartment controlled by an EG&G potentiostat (Type 273A). Thereby, the films were contacted as a working electrode by a gold wire via the FTO glass outside of the electrolyte. A platinum wire was used as counter electrode and a Hg/HgO reference electrode was utilized in 1 M KOH (+ 0.1 V vs. NHE). Iron oxide samples were cycled with 20 mV/s under the anodic conditions to 1 V(NHE) in 1 M KOH until the cyclic voltammogram (CV) curve showed steady state characteristics. CVs under dark conditions and illumination were performed. The sample was illuminated through a small orifice (0.3117 cm^2) using a 400 $mWcm^{-2}$ tungsten halogen lamp from Xenophot.

Structural characterization

X-ray photoelectron spectroscopy (XPS) XPS measurements were performed in a spectrometer by Specs with a X-ray source XR-50 and an analysator PHOIBOS Hsa 3500. The spectrometer works with Mg-K_α-radiation (1253.6 eV). The analysis was carried out by "Universal Spectrum Processing and Analysis Program" (Unifit 2011).

Spectral dependent surface photovoltage (SPV) measurements SPV measurements were performed in the fixed capacitor arrangement at modulation frequency of 8 Hz. The measurements were carried out at 0.02 mbar. A halogen lamp with a quartz prism monochromator was used for illumination. SPV signals were detected with a high impedance buffer (Elektronik Manufaktur Mahlsdorf, RC time constant larger than 1 s) and a double phase lock-in amplifier. The phase of the lock-in amplifier was adjusted with a Si photodiode which response time was much faster than the measurement period. The SPV amplitude resulted from the square root of the sum of the squared in-phase and by 90° phase-shifted SPV signals. The tangent of the so-called phase angle was the ratio between the by 90° phase-shifted and in-phase SPV signals. A phase angle of 0° corresponds to very fast charge separation and relaxation in comparison to the modulation period while the electrons are separated preferentially towards the internal surface. A change of the phase angle (values < 90°) corresponds to a change of the retardation of charge separation and relaxation.

.

Results and Discussion

Hematite thin films were prepared by the sol-gel procedure already described in our recent work (5). Shortly recapitulated; reddish colored thin layer were obtained which show in UV-Vis measurements a direct band gap transition of 2.2 eV which is typical for hematite. Structural characterization by XRD and Raman spectroscopy verifies the formation of pure hematite crystallites in the films with sizes in the range from 30 to 50 nm.

Annealing in oxygen gas flow at 500 °C

As stated in our recent publication (5), the hematite films reveal low photovoltage and small photocurrents with respect to the oxygen evolution reaction (OER). From UV-Vis measurements it is concluded that charge carriers are generated by visible light absorption at a wavelength ≤ 573 nm. Apparently, these generated charge carriers cannot participate in the reaction. It is assumed that high recombination rate of excited electron-hole pairs and/or trapping of the holes cause the low photoactivity of the electrodes. From the literature, it is known that post-preparative annealing leads to an improvement of the crystallinity, so that defects and traps in the crystal lattice can be reduced. Therefore, in our first approach post annealing of the films was performed in oxygen gas flow at 500 °C for two hours. In figure 1 the cyclic voltammograms (CV) of the hematite film before and after the annealing step are presented.

In contrast to the pristine film, the anodic current of the annealed film under dark conditions is shifted to a more positive potential by about 130 mV. It is assumed that the dark reaction is initiated by charge carriers via intermediate surface states located near

the valence band. These surface states seem to be reduced due to the annealing step. Thus, Fermi level has to be shifted to more negative potentials in order to initiate the reaction.

In addition surface states seem to be reduced due to the annealing step so that more energy is necessary to shift the Fermi level and thus to initiate the reaction.

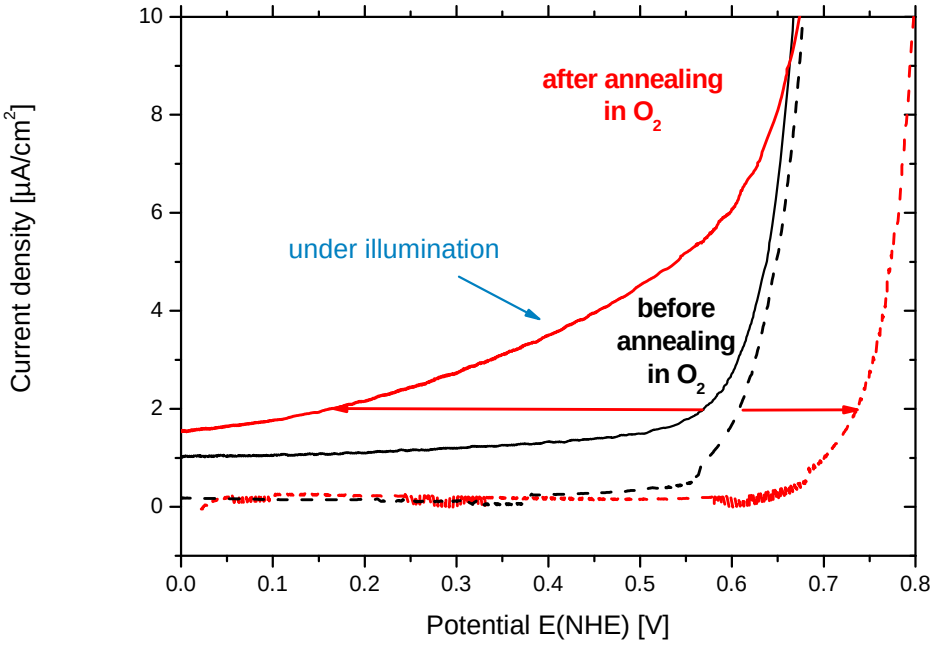

Figure 1. CV measurements of the pristine (black) and annealed hematite layer (red) prepared from the sol-gel procedure in 1 M KOH with 20 mV/s (0.3117 $cm^{2)}$ under dark conditions (dotted line) and under illumination (solid line).

The enhanced supply of generated and separated charge carriers by the photoabsorption due to the annealing is also observed in the onset potential of the photo-induced oxidation current. For the evaluation of the obtained photoactivity the potential at 2 $\mu A/cm^2$ is used. This potential is addressed as onset potential in the following analysis.

After the annealing step the onset potential is shifted from 570 to 160 mV(NHE) due to the higher generated photovoltage. This photovoltage is determined by the difference of the onset potentials in the dark and under illumination. After annealing the intern generated photovoltage is increased from 30 to 580 mV. This can be explained by a diminished recombination rate in the bulk and at the surface and/or by a more efficient charge-carrier separation rate of the photoabsorber under illumination assuming different Fermi level positions in the bulk and in surface near regions.

In our recent publication, it was found by TEM analysis that the crystallinity of the films is changed by the heat treatment (5). XRD analysis reveals a significant increase of the (110) diffraction line of the annealed samples which indicates either a preferential reorientation of the crystallites, with respect to the substrate, or a changed crystal shape, with an increased number of (110) lattice planes belonging to the individual crystallites. Although the impact of this effect on the electrochemical behavior is not clarified it could in addition be a reason for the improved photoactivity.

Therefore it is concluded that – beside passivation of surface states and an assumed shift of the Fermi level position near the surface – coalescence and oriented intergrowth of the crystallites also contribute to the improved semiconductor properties. Obviously, defects in the bulk are removed so that an increased photovoltage can be built up under illumination and a higher rate of excited charge carriers are additionally provided at the electrode/electrolyte interface for the pursued electrochemical oxygen evolution reaction.

Oxygen plasma treatment

Nevertheless, the post-annealed hematite film only reveals a low photocurrent although a pronounced photovoltage is obtained. For an efficient water oxidation reaction at the electrode/electrolyte interface, electrochemically active structures on the hematite surface need to be available for the reaction. Apparently, these catalytically active structures are missing. An approach to activate the chemical interface was a treatment of the pristine hematite films in oxygen plasma.

In figure 2 the CV curves before and after the plasma treatment are presented.

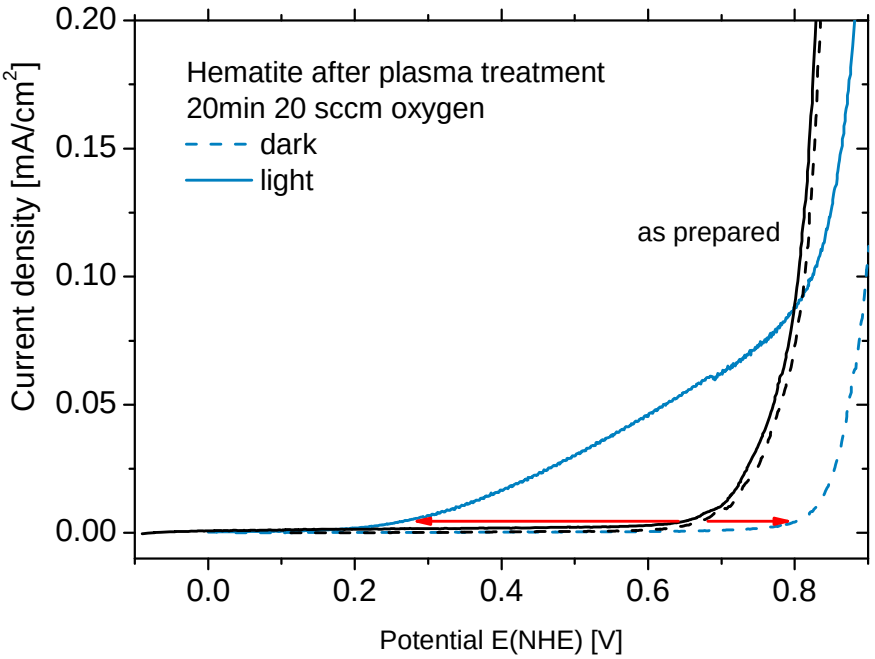

Figure 2. CV measurements of the pristine (black) and a plasma treated hematite layer (blue) prepared from the sol-gel procedure in 1 M KOH with 20 mV/s (0.3117 cm^2) under dark conditions (dotted line) and under illumination (solid line).

Electrochemical analysis reveals a significant improvement of the photoactivity after plasma treatment which is very similar to the effect observed with heat treated samples as it is shown in figure 1.

Again the dark current is shifted by 100 mV to an onset potential of 760 mV(NHE) (at 2 $\mu A/cm^2$) and the onset potential of the photocurrent is shifted to 200 mV(NHE) (at 2 $\mu A/cm^2$) which is comparable to the heat-treated samples. Furthermore, the obtained photovoltage calculated from the difference between the onset potentials in the dark and under illumination (560 mV at 2 $\mu A/cm^2$) is similar to the annealed sample.

We suggest that these improved photoelectrochemical properties obtained by the plasma treatment can be attributed to the similar physical changes that also occur by the annealing step (discussed above). Although the plasma treatment is known as a surface treatment method, changes of the bulk evoked from the plasma are also considered in this case. A notable thermal energy entry also occurs during the plasma treatment. Nevertheless, it is difficult to evaluate, how the crystallinity and the resulting recombination rate are affected.

A remarkable difference between the annealed and plasma-treated sample is seen in a significantly increased photocurrent after the plasma treatment. In contrast to the annealed sample the photocurrent for the plasma-treated sample increases more pronounced with increasing potential. At 0.5 V(NHE) a photocurrent of 30 $\mu A/cm^2$ is detected while the annealed sample only achieves 4 $\mu A/cm^2$ at this potential. Because of the similar photovoltage, it is concluded that a different hematite interface is generated by the plasma treatment which reveals structures with more beneficial catalytic properties for the water oxidation reaction. This might be reasoned in the use of highly reactive oxygen species in the oxygen plasma which attacks and modifies the hematite surface.

XPS analysis was performed in order to investigate the structural changes caused by the plasma treatment. Generally it was noted that the oxygen concentration is increased from 49 to 86 at-% on the surface of the sample. Apparently, oxygen is introduced in the surface layer. Remarkable changes were detected in the O1s spectra of the untreated and treated sample, as shown in Figure 3.

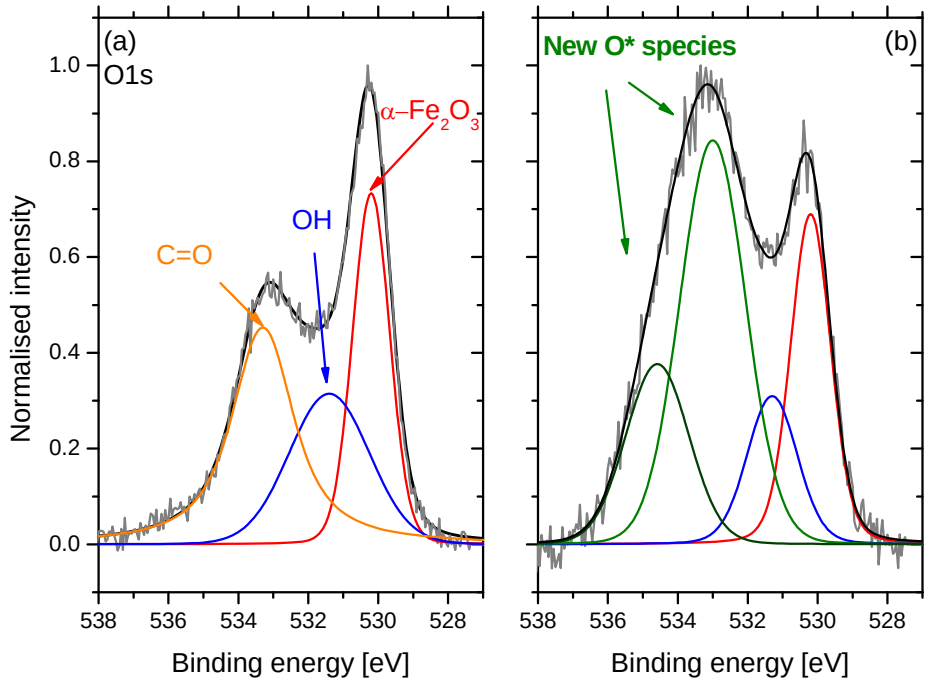

Figure 3. (a) O1s spectra of the untreated and (b) the plasma treated hematite layer prepared from the sol-gel procedure.

The untreated sample shows in the O1s spectra three peaks fitted in the spectra. The peak at 530.2 eV is attributed to the hematite (7, 8). The peak at 531.4 eV is identified as OH surface groups of the iron oxide (9). Finally the peak at 533.3 eV is allocated as

carbonyl-type CO ligands or adsorbed carbon dioxide (10). After the plasma treatment the latter one disappears. Instead, new oxygen species with high intensity at 533 and 534.6 eV were detected. On the origin of these peaks can only be speculated. Due to the high binding energy it is assumed that these new oxygen species are double bonded oxygen (O=O) species or encapsulated H_2O groups (11).

It is assumed that these new oxygen species incorporated at the surface by the plasma treatment are responsible for the increased photoelectrochemical activity towards water oxidation.

Successive post-treatment

As the heating effect during the plasma treatment is not well defined and furthermore is coupled to the plasma power and therefore to the extent of the surface modification in further experiments, a separate thermal annealing in a first step and a subsequent plasma treatment was applied to the samples, in the same procedure as described above.

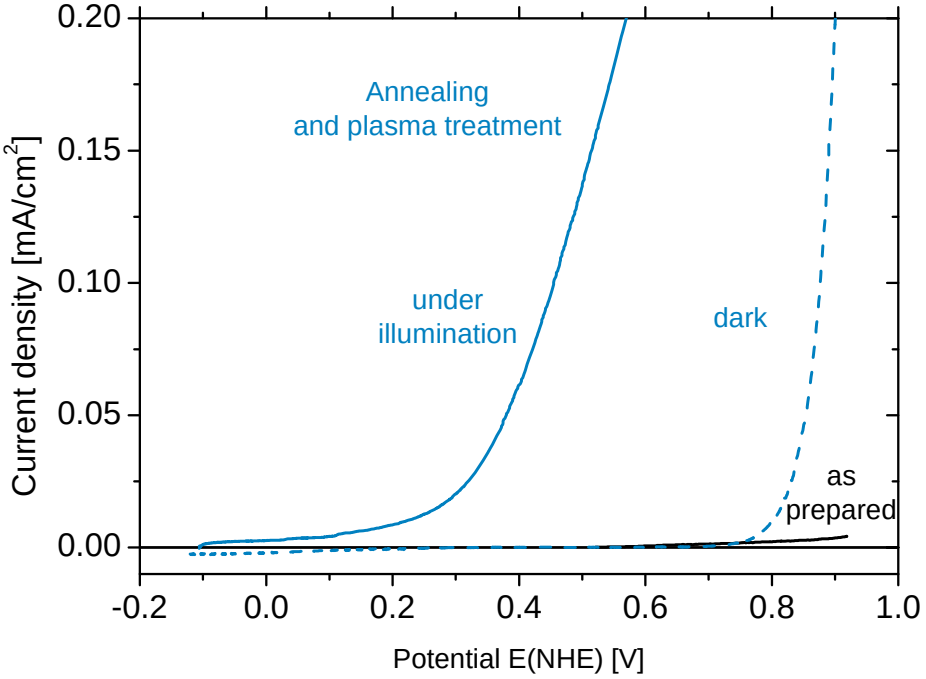

Figure 4. CV measurements of a successively treated hematite film: as prepared (solid black line) under illumination and after thermal annealing and plasma treatment in 1 M KOH with 20 mV/s (0.3117 cm^2) in the dark (dotted blue line) and under illumination (solid blue line).

Figure 4 presents the CV curves before and after the post-treatment process (combined thermal annealing and plasma treatment). The pristine hematite film formed by the sol-gel process reveals a low photoactivity, as already mentioned above and in our recent publication (5). After the heat treatment in oxygen gas flow at 500 °C and a subsequent plasma treatment the onset potential of the photocurrent is shifted to about -

70 mV(NHE) (at 2 µA/cm^2). This is significantly more negative compared to the single plasma treated and annealed samples whose onset potential is about +200 mV(NHE). The calculated photovoltage from the CV is determined to 830 mV.

The slope of the photocurrent is also increased. At 0.5 V(NHE) a current density of 0.13 mA/cm^2 is yielded. This is four times higher than for the (single) plasma treated sample. The exponential course of the photocurrent indicates that the current is mainly limited to the electrochemical kinetics of the reaction and no longer by the dynamics of the charge carriers in the semiconductor.

Besides an increased photovoltage, a more reactive hematite interface is present after this combined post-treatment procedure compared to a single plasma treatment. It is suggested that the annealing procedure before the plasma treatment leads to a beneficial orientation of the hematite crystallites in the layer, as after the single annealing procedure. In contrast to that the single surface-sensitive plasma treatment cannot lead to a reorganization of the bulk but only to the surface near parts of the layers. Nevertheless, the interface subjected to the plasma treatment seems to be changed compared to the plasma treatment without the annealing step before. The improved catalytic properties of the obtained sample indicate that a more reactive structure can be achieved by this combined procedure.

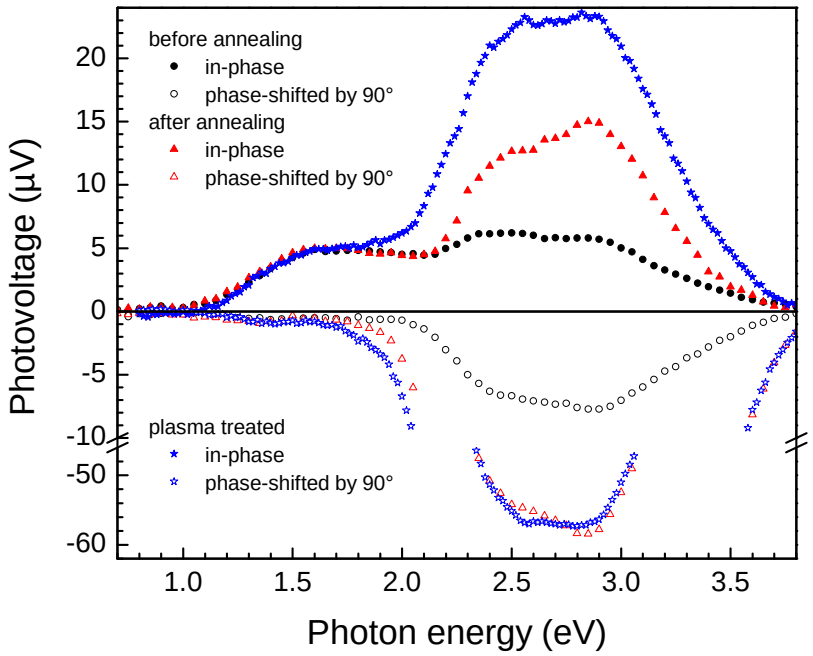

Figure 5. Surface photovoltage spectra of the in-phase (filled symbols) and phase-shifted by 90° (open symbols) signals of a hematite film deposited on a SnO_2:F coated glass substrate measured before (circles), after (triangles) annealing in oxygen atmosphere and after oxygen plasma treatment (stars).

This successive improvement is also mirrored in surface photovoltage measurements (SPV). Figure 5 shows typical in-phase (x) and phase-shifted by 90° (y) SPV spectra of the untreated α-Fe_2O_3 nanoparticles in the film as well as the counterparts measured after annealing in oxygen atmosphere and after the plasma treatment, respectively. As long as

the x-signals are positive, the electrons were preferentially separated towards the internal surface. The SPV signals set on at photon energies of about 1 eV. A similar onset of charge separation at defect states was observed also in optical absorption spectra (absorption coefficient below 10^3 cm^{-1} (12)). The x-signals increase steeply at a photon energy ranging from 2.15 to 2.2 eV which can be correlated to the band gap energy of α-Fe_2O_3. In the defect region, the y-signals were by about one order of magnitude smaller than the x-signals whereas the y-signals were larger than the x-signals in the region of fundamental absorption of hematite. The x- and y-signals in the defect range remained practically constant while the signals increased in the region of fundamental absorption after annealing. Interestingly, the sharp onset of the y-signals appeared at about 2 eV, i.e. at an energy significantly less than for the x-signals. Further additional y-signals appeared between 1.7 and 2 eV after annealing.

After the plasma treatment the in-phase (x) signals at 2.1 to 2.5 are further increased. This indicates an increased charge carrier generation and separation from the band-gap transfer. The in-phase spectrum of the plasma treated sample also reveals an increase of the signals below the band gap compared to the one of the annealing step. This contribution presumably originates from an increase of states due to stress in bonds close to the surface. Because this photovoltage fraction is only observed for the plasma-treated sample, it is assumed that the transfer to the new oxygen species on the surface evoked by the plasma treatment is responsible for this photovoltage contribution.

The analysis of the phase angle spectra opens the opportunity to distinguish charge separation from different defect sites below the band gap (2.3 eV). The phase angle spectra of the samples presented in figure 5 are given in figure 6. The phase angle (φ) changed from -15° at 1.25 eV to -6° at 1.55 eV for the as prepared and annealed samples. The phase angle remained practically constant between 1.55 and 2.00 eV, increased steeply between 2.00 (φ = -8°) and 2.3 eV (φ = -40°) and increased moderately up to -55° at higher photon energies for the as-prepared sample. Additional spectral features appeared for the annealed sample in the defect range. The value of φ changed moderately from -8° at 1.7 eV to -26° at 1.95 eV, increased steeply to -74° at 2.15 eV and remained nearly constant at higher photon energies.

The phase angle is highly sensitive to any change of transport and recombination processes. At least one of the excited charge carriers should be mobile within the charge separation length for separation and transport. Charge separation from deep surface states and relaxation back (region A in figure 6) has other characteristics than similar processes from shallow traps (region C) or band states (interband transitions, region D). Surface and bulk defect states cannot be clearly distinguished for region A. The SPV signals strongly increased after annealing for excitation at photon energies above the band gap. This can be interpreted in terms of an increased band bending due to an increased concentration of occupied surface acceptor states and consequently due to an increased charge separation length.

Signatures of bulk defect states, which are known from optical absorption measurements, were detected by SPV and additional related defect states appeared after annealing (see region B in figure 6). Therefore, annealing led to significant structural changes within the charge separation length. The onset of region B shifted to lower photon energies and the absolute value of the phase angle of region D decreased after plasma treatment, i.e. the change of bond configuration to increased stress in bonds close to the surface caused a faster response of the modulated SPV.

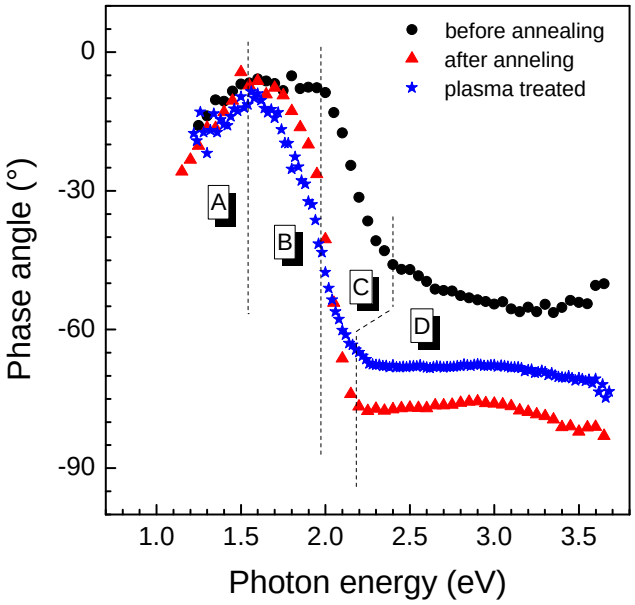

Figure 6. Phase angle spectra of the sample given in figure 5 before (circles), after (triangles) thermal annealing and after plasma treatment (stars). A, B, C, D mark regions of characteristic transitions.

Conclusion

Charge-carrier recombination and trapping processes were hypothesized as reasons for low photoelectrochemical activity towards the water oxidation reaction for hematite photoanodes prepared by a cost-efficient sol-gel procedure. A subsequent annealing step of the hematite films in an oxygen gas flow at 500 °C for two hours leads to improved photoelectrochemical properties. The onset of the photo-induced current is shifted by 570 mV to more negative potentials. In our recent work (5) a reorganization of the hematite nanoparticles in the film to a preferential (110)-texture was observed by TEM and XRD analysis. Surface photovoltage measurements (SPV) indicate an increased charge-carrier separation originating from band to band transition. During the annealing process a re-crystallisation of the hematite nanocrystals in the film takes place in which bulk defects are apparently reduced.

A successive oxygen plasma treatment after the annealing step leads to a significantly increased photocurrent. Thereby it was shown that the beneficial surface treatment by plasma can be combined with the improved crystallinity of the hematite film particles after heat treatment. From structural investigation, it was found that an oxygen enriched surface is formed during plasma treatment. Furthermore new oxygen species are detected by XPS analysis which are correlated to the improved catalytic surface properties. SPV measurements identify the formation of new surface states close to the valence band which are believed to be responsible for the enhanced charge transfer kinetics across the electrode/electrolyte interface in the water oxidation reaction.

Acknowledgments

Financial support of the BMBF under contract # 03SF0353A "H_2-NanoSolar" is gratefully acknowledged. The authors would like to thank Dr. Gledhill for careful reading of the manuscript.

References

1. S.D. Tilley and M. Cornuz, *Angewandte Chemie Int. Ed.*, **49**, 1 (2010)
2. R. van de Krol and M. Grätzel, *Photoelectrochemical Hydrogen Production*, Springer US, New York page 121 (2012)
3. K. Sivula, F. Formal and M. Grätzel, *ChemSUSChem*, **4**, 432 (2011)
4. C. X. Kronawitter and S. S. Mao, *Applied Physics Letter*, **98**, 092108 (2011)
5. I. Herrmann-Geppert and P. Bogdanoff, *ECS Transactions*, **41** (33), 201 (2012)
6. M. P. Pechini, US Patent No.3.330.697 July 1st (1967)
7. T. Fujii and F.M.F de Groot, *Physical Review B*, **59**(4), 3195 (1999)
8. J. L. Junta-Rosso and M. F. Hochellla Jr., *Geochimica et Cosmochimica Acta*, **60**(2), 305 (1996)
9. J. Haber and J. Stoch, *Journal of Electron Spectroscopy and Related Phenomena*, **9**(5) 459 (1976)
10. K. Kinoshita, *Carbon: Electrochemical and Physicochemical Properties*, John Wiley & Sons, Berkeley (CA), page 116 (1988)
11. NIST XPS database, http://srdata.nist.gov/xps/ (last access: June, 15th, 2012)
12. L. A. Marusak and R. Messier, *J. Phys. Chem. Solids*, **41**, 981 (1980)